CONTROLLING THE MICROSTRUCTURE OF ARC SPRAYED SHELLS

P. S. FUSSELL
Alcoa Laboratories
Alcoa Center, Pennsylvania 15069 USA

H. O. K. KIRCHNER
Institut de Sciences des Matériaux
Université Paris-Sud F 91405 Orsay, Cedex, FRANCE

F. B. PRINZ
Engineering Design Research Center
Carnegie Mellon University
Pittsburgh, Pennsylvania 15213 USA

L. E. WEISS
Robotics Institute
Carnegie Mellon University
Pittsburgh, Pennsylvania 15213 USA

13 May 1991

Abstract—Techniques for controlling the microstructure of sprayed steel structures are discussed in this paper. Steel is arc sprayed onto shaped substrates to form tooling. The quality of the tool is greatly influenced by the microstructure of the material and the inter-lamella regions of the deposit. This work is focused on characterizing the microstructure, improving the state of the inter-lamella regions, and discusses our success in forming pseudo–alloys and graded shells by mixing sprayed materials. Microstructure control has interesting implications for other research as well, such as the MASK & DEPOSITS approach of forming objects.

1. Rapid Tooling

Rapid manufacturing of tooling for injection molding, stamping, composite layup or similar processes where the shape of the tool is critical is a challenging problem with considerable commercial potential [1]. The creation of such tooling by arc–spraying zinc and zinc alloys has been in the commercial literature for at least 25 years [2], and thick sprayed zinc structures have been in the literature for 65 years [3]. These alloy systems, however, are relatively soft and prone to wear and loading failure; their usefulness is largely limited to prototype tooling applications and low pressure applications such as reaction injection molding tooling. Tools made from ferrous systems[4, 5], as shown in Figure 1, are of far greater applicability, both for superior prototyping and limited production. They present much greater wear resistance compared to zinc systems, they are stronger, and they withstand the demands of elevated temperature service. Further, the demands of the injection molding application are well matched to the ferrous shell structures produced by arc–spray, particularly the support of hoop stresses in the tool structure, the tolerance of compression in the the ferrous shell, and the tool face wear resistance to abrasive plastics such as glass filled nylon.

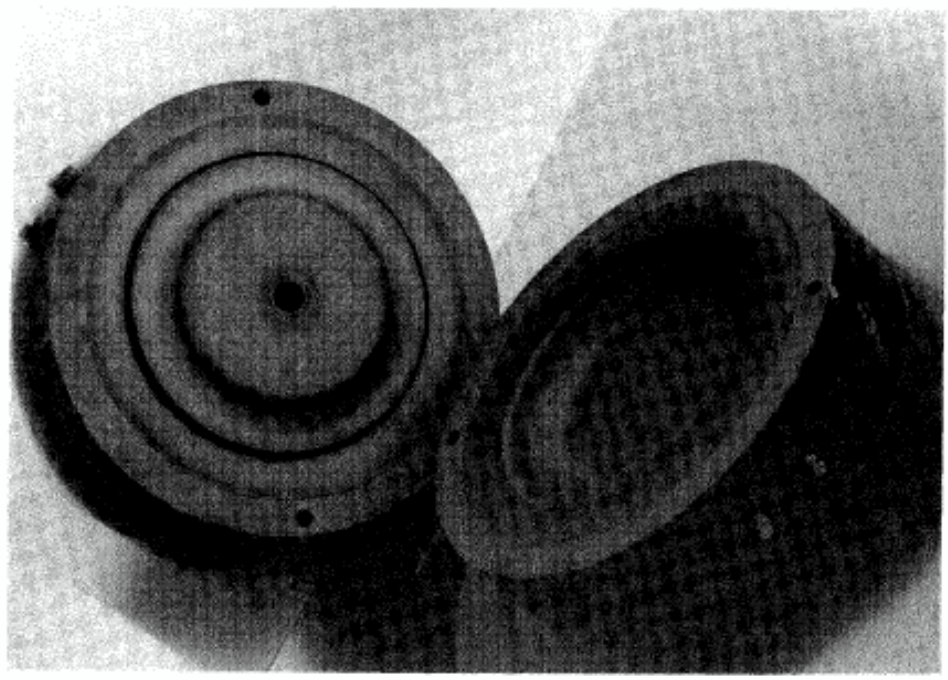

Fig. 1. A 420 stainless steel sprayed injection mold for a flying disk.

Our system uses a computer based geometric modeling system (NOODLES [6]) to describe the part and patterns needed to make the part's mold or die. A solid freeform fabrication process, a stereolithography apparatus† in this case, autonomously creates the pattern in a matter of one or two days. The shells are fabricated by robotically spraying metal using an arc–spray device to create the tooling face and structure. The back side of the tooling cavity is then filled with a support material to sustain the compressive service loads. Figure 2 shows a cross section of such a tool.

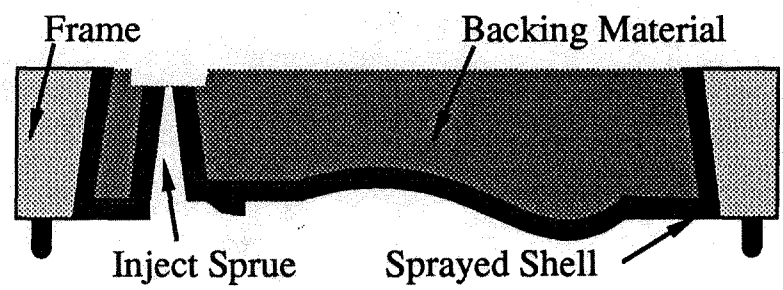

Fig. 2. Schematic cross section of a sprayed tool.
The frame interior is angled to help support compressive loads on the tool face.

† Stereolithography has been commercialized by 3D Systems, Inc. of Valencia, California under US Patents 4 575 330 B1, and 4 929 402.

The synergy of a coherent, computer based three-dimensional modeling system, a rapid prototyping fabrication device, and robotically based spraying system has made this approach for manufacturing low volume tooling economically appealing, particularly for geometrically complex shapes: the time needed to manufacture such a tool is of the order of one week; and the cost of the manufactured tool is substantially less than a conventionally made one-of-a-kind mold or die.

The direct linkage of the part's computer model and the part's tooling results in paperless manufacture; changes in the part's geometry are directly communicated to the next iteration of tooling, and unacceptable aspects of the design, from a manufacturing perspective, are communicated back to the part's computer model. Using the robot to manipulate the arc–spray gun has three striking advantages: any particular schedule for spraying a mold or die half is repeatable; moreover the robot is precise, meaning, for example, an intended standoff of 10 cm is precisely executed; and the robot is reprogrammable for new tooling designs. This combination yields immediate benefits in the quality of sprayed ferrous alloy shells. The robotic repeatability is required for consistency in the sprayed shell, as well as consistency in this experimental work. The robot, being a programmable mechanism with considerable freedom of motion, is also capable of spraying complex surface geometries.

The basic fabrication of these sprayed ferrous tools had been problematical. In making sprayed tooling, metal is first sprayed onto a substrate, and then removed from that substrate; thus the interface layer between substrate and coating is by design weak in order to permit that separation.

After the arc-spraying is completed, the shell and the substrate still contain considerable internal stress, albeit in equilibrium. These thermally induced stresses can be very large [7]. When the shell is separated from the substrate, the shell deforms as it comes to a new equilibrium. Our current process art limits this to roughly 1 mm deflection in 500 mm length of shell for a 2 mm thick shell. Secondly, the sprayed shells are backed with a mass castable ceramic or filled epoxy to principally provide tool compressive strength. If the shell and the backing material have different coefficients of thermal expansion, then the normal thermal cycling of a tool will create shear at the shell, backing interface. The presence of internal stress in the shell, as well as a mismatch of coefficients of thermal expansion, also raise questions of the shell's geometric stability at elevated temperatures, and over long times. Finally, the spray process is poorly suited for spraying into narrow channels and small aspect ratio holes.

As much of the tool's function is determined by its geometry, much of the tool's strength and wear characteristics are determined by the microstructure of the sprayed shell. The focus of this work is the microstructure of the sprayed shell, with emphasis on designing aspects of the microstructure to meet the demands placed on the tool's inner shell. This is one important component of the research needed to make successful ferrous tools; this work will help guide the future efforts in the larger research program.

2. Metal Spraying Techniques

2.1 Osprey, plasma, and flame techniques..A variety of techniques are available for depositing metal by a spray process. The Osprey process [8, 9] provides large deposition rates (1000 kg hr^{-1}) by atomizing a molten stream of liquid drawn from a pool of liquid metal. This is generally done in a chamber under inert conditions. It is possible to superheat the liquid pool. The deposition rates are such that a contiguous liquid surface is present on the substrate.

Plasma systems [10-14], at the other end of the spectrum, deposit material at a rate from 0.1 kg hr^{-1} to 5 kg hr^{-1}. These systems function by propelling powdered material in a stream of gas heated by an electrical arc; gas temperatures are reported to be as high as 20 000 K [14]. Deposition rates of a few kg hr^{-1} are problematical, for typically the powder particles are not entirely melted. Plasma systems permit a wide latitude in choice of materials, as well as good of control of the resulting microstructure; they are mostly used for coating.

Flame systems, similar in concept to oxy–acetylene cutting and heating torches, melt a powder, wire, or stick of material in the flame and then use the combustion gases to blow the molten particles to the substrate. The deposition rates vary between 4 kg hr^{-1} and 20 kg hr^{-1}. As this process essentially uses a heating torch, the substrate is heated, while the particles are conveyed in a gaseous stream of combustion products.

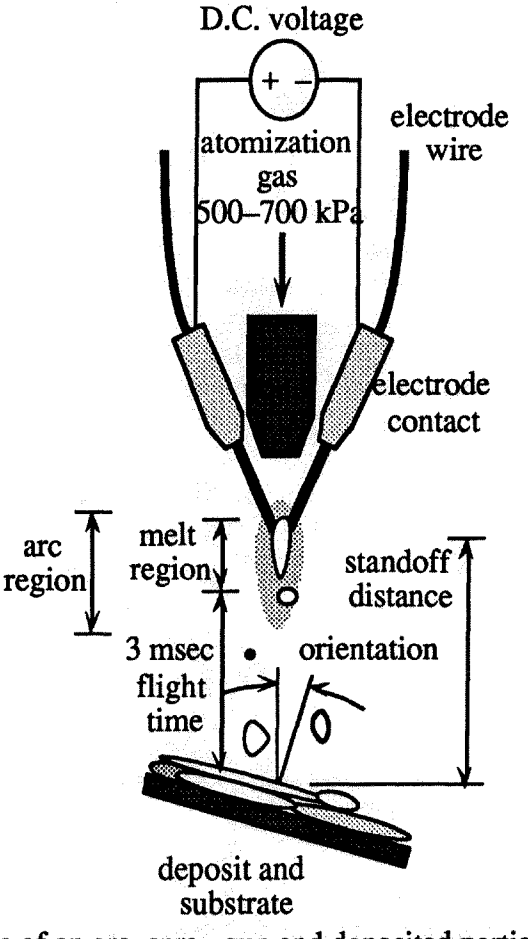

Fig. 3. Schematic of an arc–spray gun and deposited particle flight times.

High velocity variants of flame and plasma systems greatly increase the kinetic energy of the particles in order to reduce the porosity of the sprayed material. The high speed flow of molten material also serves as an abrasive to the substrate.

2.2 Arc–spray. The effort reported here uses an arc–spray system [15, 16]. It is comparable in cost to the low cost flame system while avoiding the inherent products of combustion, it is extremely easy to use, and it uses widely available materials.

The arc–spray gun is arranged as in Figure 3. Two consumable electrode wires are fed through contact tips to the area of the arc. A D.C. power supply establishes an arc between the wires, melting them in the arc. A column of atomizing gas, ranging from 480 kPa to 690 kPa (70 psi to 100 psi) ablates the molten material from the wires, atomizes the molten droplets and carries them, in a spray, to the substrate. For steel systems, the arc voltage typically ranges from 26 volts to 31 volts; the arc current ranges from 50 amps to 300 amps giving a temperature of 10^4 K in the arc [14]. Deposition rates for an arc–spray system range from 1 kg hr^{-1} to 20 kg hr^{-1}. The structures resulting from the arc–spray process are suitable for the tooling applications at hand[16, 17], and the arc–spray process permits a deposition rate that allows a timely buildup of the tool shell thickness.

2.2.1 Parameters. Within the arc–spray process, there are a number of parameters that can be controlled to affect the quality of the deposited shell [18, 19]. These principally include:

standoff distance —	the distance the particles must travel from arc to substrate;
gun orientation —	the orientation of the spray gun with respect to the substrate's surface normal, and thus the direction of impact of the sprayed particles upon the substrate;
traverse speed —	the traverse speed of the spray gun over the substrate; this directly affects the flux of particles arriving at the substrate;
gas pressure —	the atomization and accelerating gas pressure in the spray gun;
arc energy —	the energy being consumed in the arc; the resistance of the arc is essentially constant at a constant material consumption rate, so the arc power (and hence the arc specific energy) is set by the power supply voltage;
material consumption rate —	the amount of material being presented to the arc per unit time; it is specified as a feed rate of the consumable electrode. Not all of this material is deposited — a fair proportion is lost to overspray.

Table 1 shows an overview of the relationship between these parameters and some effects in the spray and shell's microstructure.

*2.2.2 Solidification and Microstructure.*Our aim is to influence the shell's microstructure indirectly by directly influencing the spray's characteristics. The porosity and oxide levels should be kept at a minimum (ideally zero), the particle sizes should be uniform, each with a uniform temperature, while imparting no heat load onto the substrate or previously sprayed shell. A measure of compromise is needed in setting the spray parameters.

The porosity in Table 1 can be most directly influenced by either increasing the particle's kinetic energy or increasing the time for coalescence on the substrate; gas pressure, standoff distance (and therefore their speed) and adding more superheat to the particles are the means to this end. Orientation has a first order effect on porosity for shadowing reasons – previously deposited particles will act as obstructions to incoming particles; worse, the hole formed in the shadow of a pre-

viously deposited particle is large, and is clustered with other such holes. Figure 4 schematically shows this effect, and Figure 16 shows the effect in the microstructure. We have found that

	Porosity	Oxide	Size of Particles	Temp. of Particles	Heat Load on Shell	Orientation of Laminae
Standoff Distance	•	o		•	•	
Torch Orientation	•					•
Travel Speed					•	
Gas Pressure	•	o	•	o	o	
Energy of Arc	o	o	o	•	•	
Material Deposition Rate	o		o	o	•	

Table 1. Qualitative effect of parameters on spray characteristics.
'•' implies first order contribution, 'o' implies a lesser influence.

orientation angles greater than 30° lead to unacceptable porosity. Oxide formation is a kinetic reaction, so, beyond eliminating or reducing oxygen in the vicinity of the molten metal or lowering the temperature of the reacting products, reducing the time for the formation of oxides is significant. Particle size is principally determined by atomization in the arc; coalescence in the arc and on the

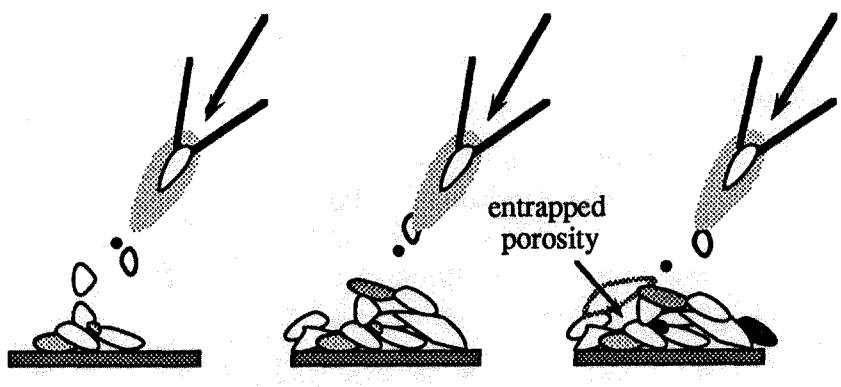

Fig. 4. A schematic of the shadow effect of porosity formation.

substrate are minor secondary factors in arc–spray. Beyond the first layers deposited, the orientation of the built-up laminar structure is controlled exclusively by the orientation of the torch.

Individual lamella morphology is a function of both the particle size, as well as the orientation of the torch with respect to the substrate's surface. The impact of the molten particles on the substrate is greatly influenced by the angle between the particle's trajectory and the local surface normal; orientations increasingly distant from the surface normal produce a more fragmented lamella. This effect, combined with the shadow effect, produces undesirable microstructural features. Naïve methods of depositing metal shells result in poor quality shells; spraying with the intention of creating sound microstructures has led us to investigate methods of making shells with lower oxide levels, lower porosity, oriented lamella, and shells built of sprayed composites.

3. Experimental Arrangement

The experimental arrangement used in this work is organized around a robotically moved arc–spray gun. Both the robot and the arc–spray system are coordinated by an IBM-AT computer; all of the experiments reported here were controlled from the IBM-AT. The arc–spray gun and power supply are commercial products (the gun is a Miller BP–400 and the power supply is a Miller Mogularc 400R); the arc–spray controller is a Miller custom built process controller that is interfaced to and controlled by the external computer which sets the wire feed rate and arc voltage, as well as starts and stops the arc process. The robot is a GMF S-700 6 axis robot, with additional degrees of freedom in a rotating table. Programs are uploaded and downloaded through the IBM-AT computer, and the IBM-AT computer initiates robotic motion. The robotic manipulator provides a high degree of motion repeatability in making the sprayed structures; the computer controlled power supply and arc–spray system gives a similar repeatability to the process variables in the sprayed structures.

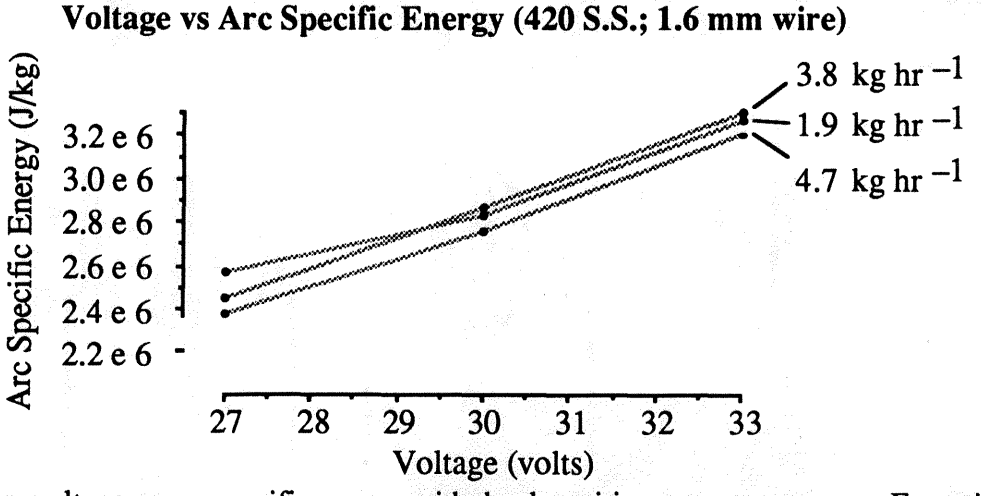

Fig. 5. Arc voltage *vs* arc specific energy with the deposition rate as parameter. Essentially the energy per unit mass melted is proportional to the control voltage, but independent of the deposition rate.

For a given deposition rate, the arc current and arc resistance are relatively constant as the arc voltage is varied; thus the power consumed in the arc is largely controlled by the voltage setting. Figure 5 shows the effect of increasing arc voltage on specific energy, all other variables held constant. With this type of equipment, this is the simplest way to increase the energy available to heat the metal particles.

The experiments were conducted at the lower end of the arc–spray parameter ranges, with a deposition rate of about 2.0 kg hr^{-1} and specific energy expenditure of 2.6 MJoules kg^{-1} (0.74 kWH kg^{-1}) of metal consumed. With the programmed torch travel speed of 500 mm s^{-1} a deposit of 0.1 mm is applied during each cycle of 24 passes. In all cases, the standoff distance was the same 16.5 cm (6.5 inches) from the arc to the substrate. Similarly, the orientation was, except as noted below, normal to the substrate (*i. e.*, the particles traveled along a course parallel to the surface normal).

The atomizing gas, in our facility, comes either from an air compressor (capable of supplying 1.2 MPa (175 psi) pressure) or from a cluster of compressed gas bottles. The process produces a broad spectrum of particle sizes, ranging from +100 micron diameter particles to sub-micron particles.

Due to the large surface/volume ratio of the sprayed droplets, oxidation in flight and after impingement is a problem. The obvious way to circumvent the detrimental effect of oxidation and avoid the ensuing brittleness of the deposit is to minimize the partial pressure of oxygen in the gaseous atmosphere [20] and keep turbulence as low as possible. The influence of these factors was studied by choosing three experimental setups, as shown in Figure 6. Either the robotically manipulated jet was directed towards the substrate without any protective cover (Figure 6a), or it was protected by a shroud (Figure 6b) that minimized turbulence of the surrounding atmosphere. In this arrangement the hot jet and the yet hot deposit is mainly flushed by the gas of the jet. Additionally an arrangement was tried (Figure 6c) where the spray gas was flushed through the shroud to provide inert gas for the turbulent mixing of the jet. The shroud is attached to the nozzle

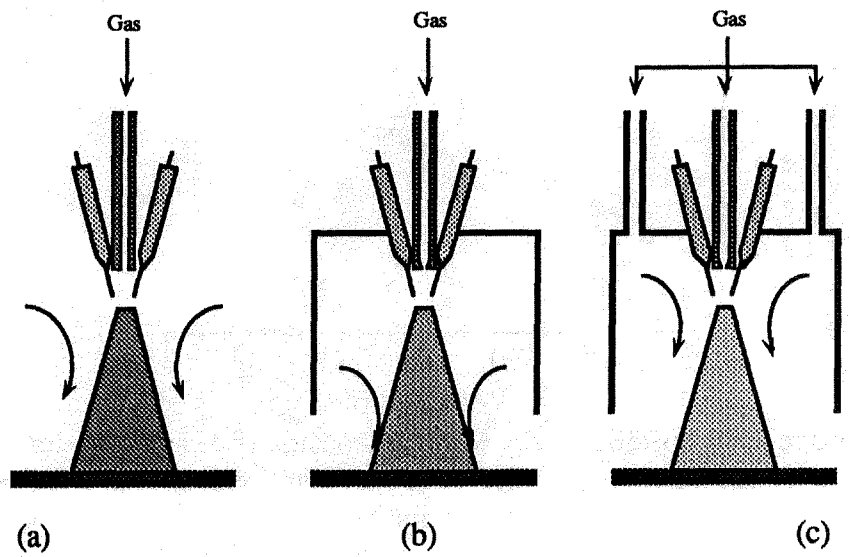

Fig. 6. Shroud arrangement for inert atomization and cover gas. (a) no protective cover, (b) protective shroud, (c) protective shroud with protective gas flow.

and moves with it. Although the distance between nozzle and substrate is kept as constant as possible in the robotic operation, there always remains a gap between shroud and substrate. Thus it is practically not possible to prevent contact between the surrounding atmosphere and the jet or the hot deposit, but obviously the shroud protects the jet rather well when and after it leaves the nozzle

(and is still slow, hot and reactive). Near the substrate turbulence might draw in some of the surrounding atmosphere, but there the temperature of the droplets and thus the rate of oxidation is already lower. In these three arrangements three different gases were used: air, nitrogen and argon. The change from the first to the second cuts down the oxygen partial pressure by a factor of five at reasonable cost, while the change from nitrogen to the heavier argon increases cost dramatically but further reduces the oxygen exposure. Further, the use of argon prevents any potential problems with nitride formation in the ferrous systems [21], and the arc is much more stable in an argon atmosphere than in a nitrogen atmosphere [22].

The metal deposition schedule for these experiments was:

Step 1. arc–spray a path consisting of 12 cycles of back-and-forth motion across a substrate (7 mm low carbon steel plate in most cases)

Step 2. wait for the temperature of the sprayed shell to return from its heated state (typically 60°C) to some nominal level (typically 40°C)

Step 3. repeat until adequate shell thickness for sectioning was reached. Generally this procedure was repeated eight to ten times, giving a typical shell thickness of 1.3 mm.

Various materials were sprayed onto mild steel that had been glass bead peened (compositions are in weight %):

(a) Plain carbon steel 1080. The composition is 0.8 % C, remainder Fe.

(b) Stainless steel 420 (a martensitic stainless steel) with a composition 0.15% C minimum, 1% Mn, 1% Si, 12-14% Cr, 0.04% P, and 0.03% S

(c) Bronze of 2% Si, remainder Cu.

(d) Invar of 36% Ni, remainder Fe.

The samples sprayed in a completely inert atmosphere were made in a closed vacuum chamber. The chamber was evacuated to 0.7 kPa (5 torr), then backfilled to 57 kPa (430 torr) with argon. The arc–spray gun was inserted into the chamber and during spraying a vane vacuum pump was used to hold the pressure at 57 kPa. The atomization gas for these experiments was argon. The substrate for these experiments was a 46 cm diameter mandrel.

4. CHARACTERIZATION OF SPRAY

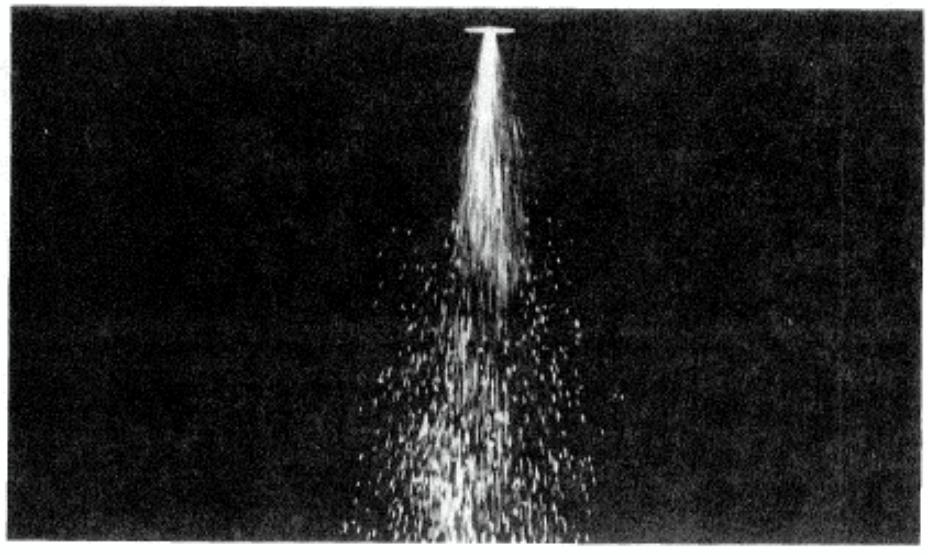

Fig. 7. Spray of 420 stainless steel in air with air atomization.

4.1 Particle velocity. Spray from the arc–spray gun is shown in Figure 7. This photo was taken with the focal plane shutter moving perpendicularly to the direction of travel of the sprayed particles; the exposure time was 250 μseconds. The photo shows the irregular nature of the arc–spray; the process sputters along rather than continuously depositing a fine shower of metal – a gap in the stream of spray is noticeable 25 cm from the arc. It is also apparent that particles along the periphery of the spray's cone are moving more slowly than those along its axis.

From the photographic evidence, particle velocity is measured to vary between 40 and 70 m s^{-1}. This speed, of course, varies as the particles leave the arc at zero velocity, accelerate in the gas stream moving at subsonic velocity, and then, as the gas stream disperses and slows, decelerate from the resistance of the gas stream. The speed of the particles should also be strongly influenced by their particular size, which, in turn, is influenced by the atomization gas pressure. Mathur [9] discusses atomized particles in a gas stream in some detail in reference to the Osprey process. As far as aerodynamics are concerned, there is little difference between the arc–spray process and the Osprey process; the velocity measurements from Figure 7 and the micrographs of section 5 show that we are in the same regime as the Osprey process: droplets of 10-20 μm diameter move at a speed of 40 to 70 m s^{-1}. Our particle flux, however, is lower and particle temperature higher.

4.2 Material buildup. The arc–spray system builds up shells by depositing particles onto the substrate. They individually splat–quench; there is never a complete liquid layer on the surface of the deposit in this process at the material deposition rates under consideration. The deposit is created by the buildup of these individually solidified particles. Arata [23] reports that particles in the arc–spray system cool within 125 μseconds of impact on a substrate. This suggests that these particles are cooling at least at a rate of 10^4 K s^{-1}. The resulting solidification rates are 25 cm s^{-1}. Moreau [24] has shown cooling rates in individual lamellæ of molybdenum and partially stabilized zirconia at 10^8 K s^{-1}, measuring the temperature evolution and showing that solidification is complete in 20 μseconds. This suggests solidification rates of about 150 cm s^{-1}. These high

cooling rates allow, in principle, depositing of metastable or quasicrystalline alloys which might have interesting properties [25, 26].

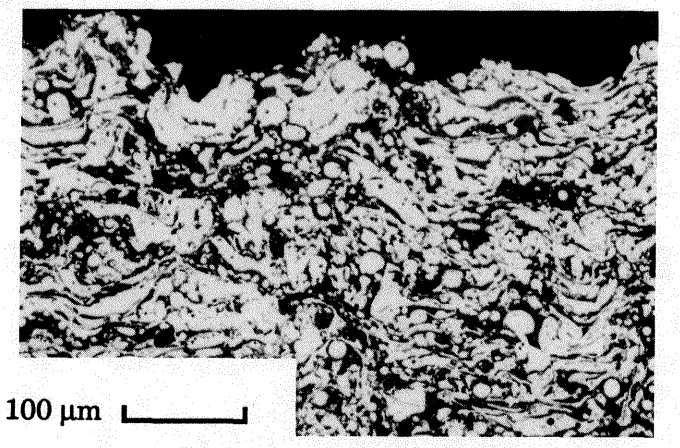

(a) Last deposited material near shell surface.

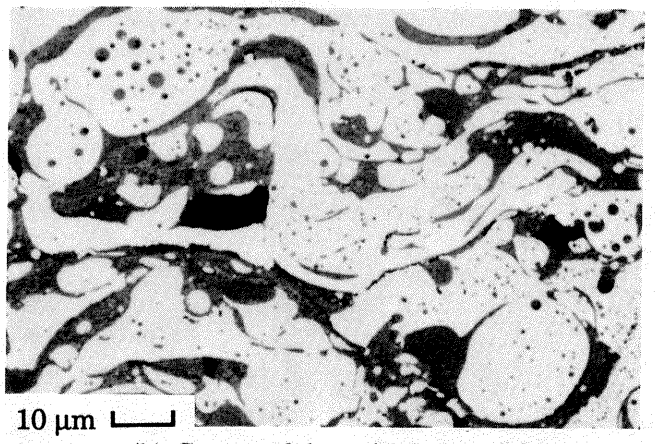

(b) Center of deposited material.

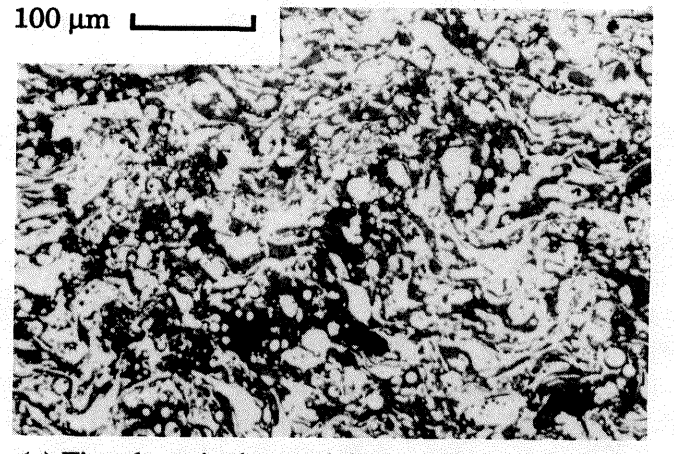

(c) First deposited material near substrate interface.

Fig. 8. Optical micrographs of cross section of 6 mm of deposited Invar.

5. MICROSTRUCTURE

5.1 Optical Metallography. In order to discuss the essential features observed, the micrograph of the Invar alloy is shown in high magnification as Figure 8 (b). This figure shows that the total deposit is built up of lamella which range from 4 to 10 μm thickness and range from 50 to 100 μm length. Each of these lamella is a solidified droplet, indicating that the average droplet–diameter ranges from 10 to 20 μm in diameter to 100 μm. The largest lamella in these micrographs suggests an original particle of perhaps 140 μm in diameter.

The micrograph indicates several things: droplets solidify in isolation – there has never been a liquid pool on the surface. The uniformity of the size distribution implies that splashing is not important: upon impinging on the surface, droplets hardly break up but flatten out to lamella before they solidify. The arc-gun was oriented so that the particles arrived normal to the surface for the material sprayed in this sample. Three different shades of gray are visible in Figure 8, particularly Figure 8(b), white, gray and black. By X-ray energy dispersive analysis, Figure 9, we verified the white area as being metal, the grey areas as oxide and the black areas as pores. The original composition of Invar is Fe–36 w% Ni; the composition has been changed in this sample by the heavy oxidation (roughly 30% of this sample is oxide). The bright regions are about Fe–40 w% Ni, and the dark regions are roughly Fe–18% Ni. Nickel oxidizes more slowly than iron, so it is unsurprising that the oxide regions are predominantly iron.

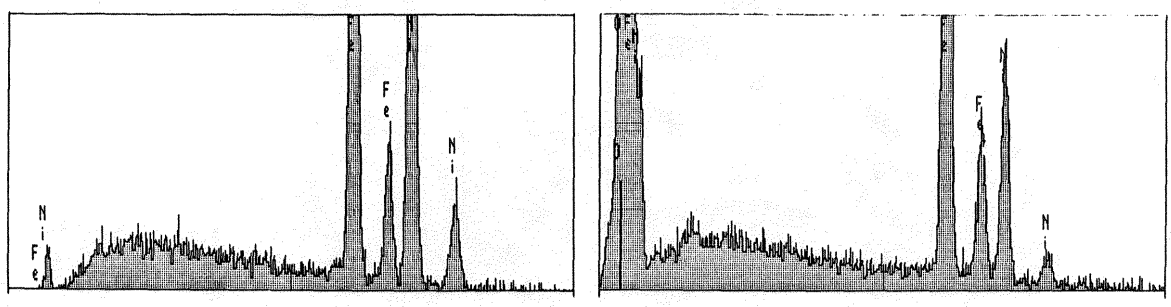

(a) Spectrum for bright (metal) regions (b) Spectrum for dark (oxide) regions

Fig. 9. X–Ray dispersive analysis of atmosphere sprayed Invar.

The morphology of the oxide particles raises the interesting question of how the formation of lamella (and not spheres) of oxide was possible. If liquid metal droplets had hit the surface, and had splat out into lamella before becoming oxidized, one would expect the lamella to be surrounded by oxide, giving a microstructure with intergranular oxide and, presumably, undesirable mechanical properties. The presence of oxide lamella indicates another mechanism: metal droplets have oxidized in the arc and in flight between the nozzle and the substrate, forming droplets of liquid oxide that hit the surface and squash out to lamella. The discussion of section 4.1 indicates that the droplets spend about 3 msec in flight, they have been heated to less than the arc temperature 10^4 K [14], but more than the oxide liquidus (1670 K for Fe_3O_4, 1830 K for FeO). Apparently these liquid iron droplets can oxidize to liquid Fe_3O_4, Fe_2O_3, and FeO while being kept well superheated for 3 msec.

5.2 Oxide. The oxide and porosity levels in the deposited shells are shown in Figure 10 with micrographs of these shells. The oxide and porosity measurements shown here have been performed using an image analysis program analyzing scanned images from photomicrographs. The

level of uncertainty in these measurements is high. Fowler [27].has shown that with eight repetitions on a single sample, it is possible to operate within a 95% confidence band for porosity measurements, but oxide measurements require more measurements. This can be seen in this data in the 0.8%C – Fe column; the oxide and porosity values vary in unexpected ways compared to the other materials. Further, spray-gun designs greatly influence the porosity and oxide levels in the sprayed shell. The measurements here, therefore, should only be used to represent what trends are possible with inert gases.

With the open unprotected arrangement of Figure 6a one obtains an oxide content of approximately 30% for both steels and the Invar alloy if air is used for atomization. This drops to 10% to 15% oxide for a nitrogen atomization gas in an air environment. If oxidation had occurred only in the nozzle, no oxidation should have occurred at all, but the turbulence of the air-atmosphere still causes oxidation. This is largely prevented by using the arrangements of either Figure 6b, or better still, Figure 6c. These decrease the oxide content to about 8%. If argon is used in the nozzle with the protection of Figure 6b or 6c, the oxide content falls to less than 8%. If the experiment is conducted in a vacuum chamber backfilled with argon, the oxide content drops to less than 2%, but this arrangement is experimentally expensive. In the argon backfilled chamber, the measurement of oxide reflects wire contamination more than in-spray formed oxide.

5.3 SEM Metallography. Figure 11 shows a backscatter image of the sprayed eutectoid steel (0.8% C). Depending upon the quench rate of the material, and the temperature history of the material, several phases and mixtures of phases are possible: pearlite, a mixture of ferrite (α) and cementite (Fe_3C), upper bainite, lower bainite, martensite, and retained austenite (γ) [28]. For this composition of steel, pearlite and the bainite transformations can be avoided if the cooling rate from 996 K to 473 K is at least 200 K s^{-1} [29]. If the cooling rate is much faster, martensite particle formation will be suppressed as well [30, 31]. The 25 μm particle in the center of Figure 11 shows an already solidified particle when it arrived at the substrate. This particle is entirely composed of retained austenite. The lamella below and surrounding the particle arrived at the substrate in a molten state, and subsequently solidified. The cooling of this lamella was such that martensite particles formed in the last deposited, or upper, portion of the lamella, while the lower region of the lamella is only retained austenite. This shows the cooling rate was highest near the lamella-substrate interface, and that the region of the splat away from the interface stayed longest at high temperature. The lamellæ and particles in this figure probably arrived at the substrate nearly simultaneously; the solidified particle forced itself onto the previously arrived lamella, forcing the liquid surface up and around. In the larger lamella of Figure 11, small pores, of the order of 0.1 μm to 0.5 μm in diameter, are also visible. These appear in all of the sprayed materials from this process, and are an artifact of the violence of the ablation and atomizing processes.

The microstructure in the lamella of arc–sprayed material is the same as the structure of splat–ribbon materials, while the interfaces between the lamellæ are much worse. This is the problem of the process. The production of splat-ribbons is a continuous casting process. The arc-spray process deposits liquid droplets individually on the solid surface, each of these droplets undergoes thermal stresses during cooling and this can lead to decohesion or microcracking along the lamella-lamella interface. The usual consolidation methods, like HIP or forging (cold or hot working) are in conflict with our intentions for this sprayed material, and therefore more subtle methods like laser glazing or shot peening of each layer could and should be used. For the unconsolidated deposits

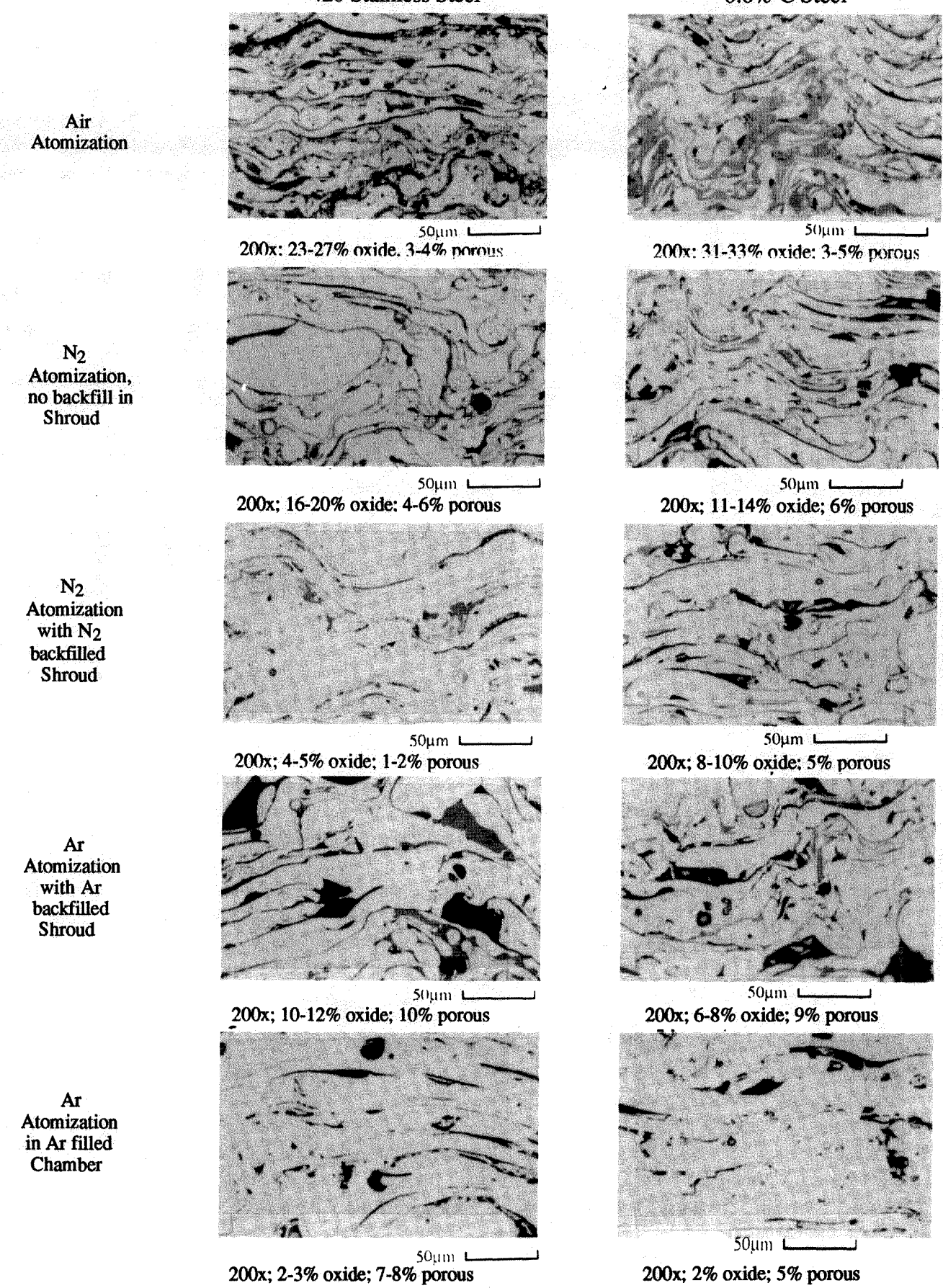

Fig. 10 (a) shows metallographic sections of the 0.5% C steel and 420 stainless steel deposits

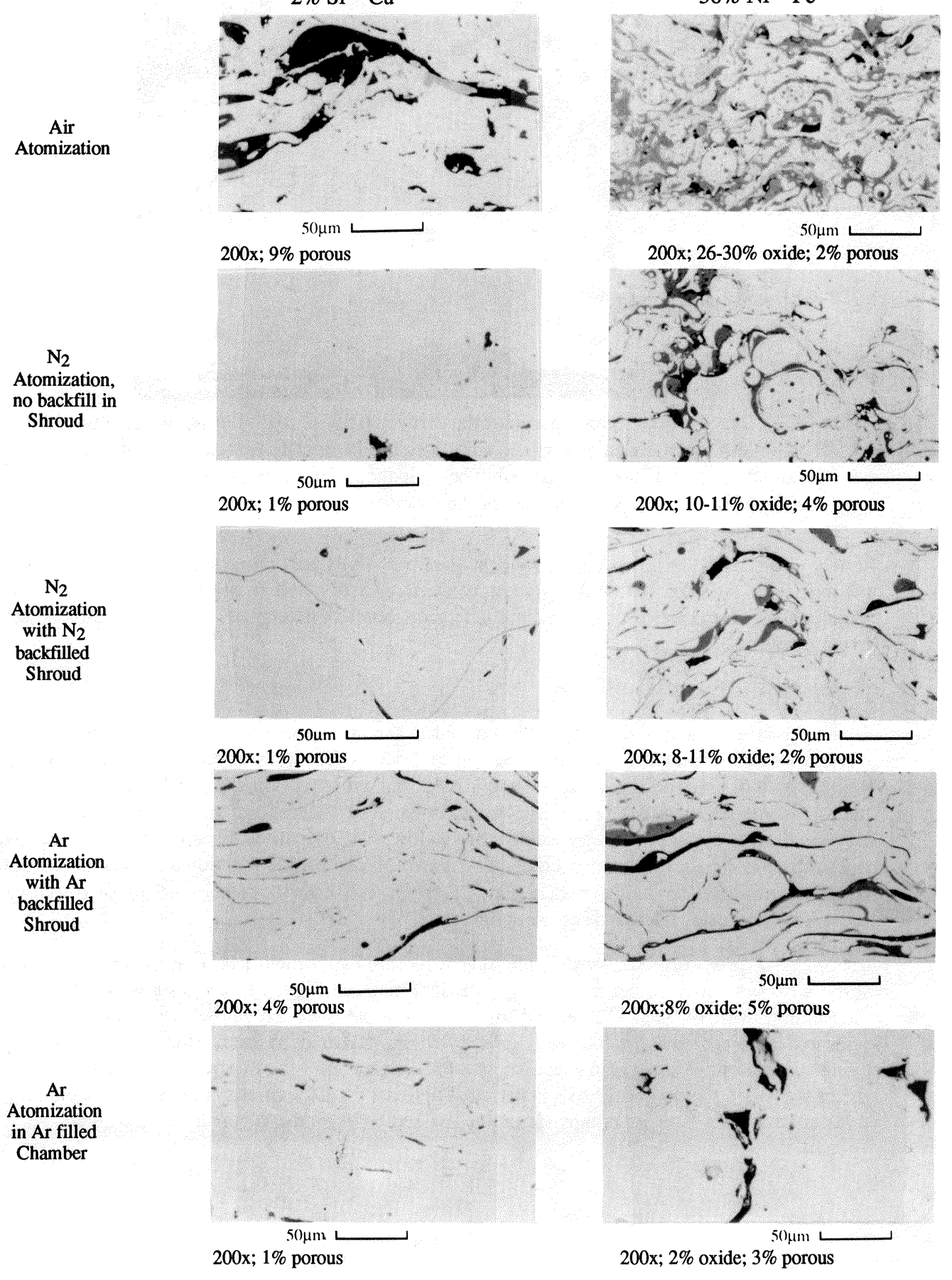

Fig. 10 (b) shows metallographic sections of the Copper and Invar deposits

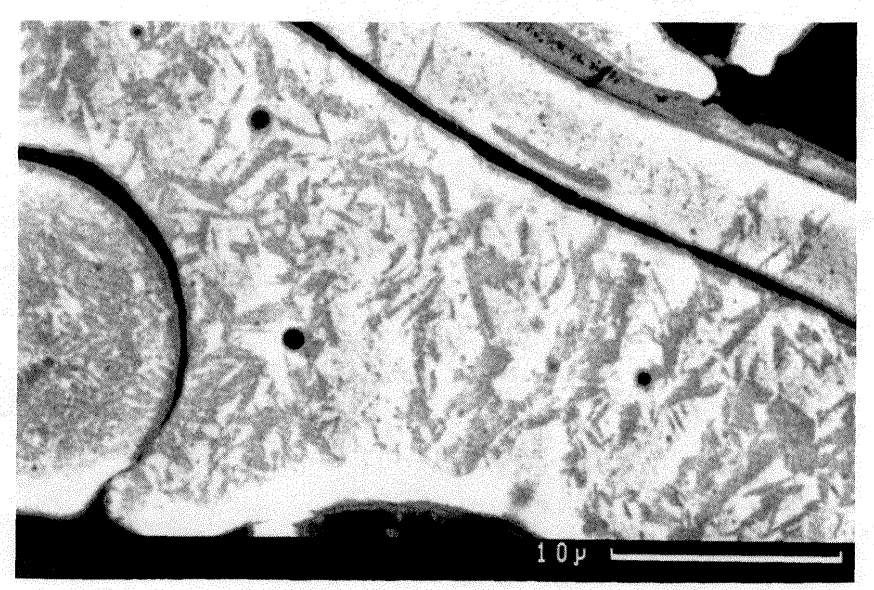

Fig. 11. SEM microphotograph of the sprayed 0.8% C steel; Showing martensite formation surrounded by retained austenite. The martensite particles are acicular in appearance in this section (probably being lenticular in three dimensions) and vary in size; they are of the order of 0.5 μm by 4 μm.

shown or discussed in this paper, the mechanical properties are controlled not by the behavior of the individual lamellæ, but by the strength of the interfaces between them. The presence of inter-lamella microcracks might be detrimental in tension, but is of no concern for metal shells subjected to compression.

6. Composite Structures

Given the layered and disjoint lamellæ formed in the arc–spray process, even when sprayed in oxygen free environments, we are motivated to develop processes to control the microstructure without cold or hot working the entire shell. As discussed in section 2.2.1 and Table 1, there are a number of process parameters that can be manipulated to affect the particles forming the lamella. Beyond the arc–spray process parameters, we follow two compatible directions: control the material properties by altering the materials deposited, and control the position and orientation of the lamella to improve the shell's characteristics. Our goal is to tune the material in the shell so it more successfully meets the demands of the application.

6.1 Sprayed Composite Materials One microstructure experiment has been to create a stratified shell, with each stratum being made of a distinct material.Figure 12 shows a structure made of alternating layers of 0.8% C steel and Invar. The sample has been etched with picral for 15 seconds to darken the steel. Each layer is about 0.15 mm (0.006 inch) thick. This sample was sprayed using argon atomization gas, a shroud, and a backfill shroud gas of argon. Figure 13 shows a detail of the mixing region of the two materials. There are no difficulties in the inter-layer bonding of this material, even though perhaps 15 minutes passed between the deposition of the layers.

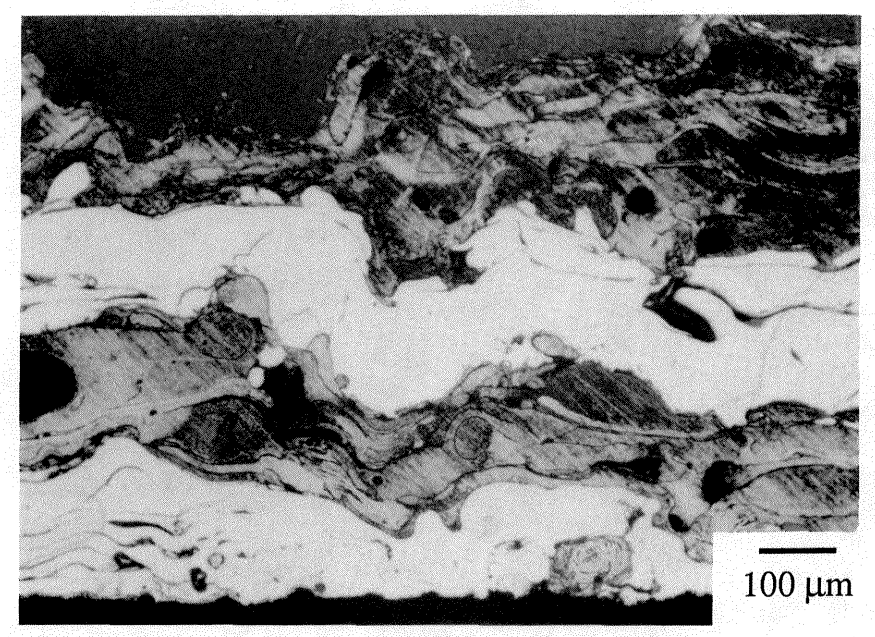

Fig. 12. Composite layered structure of 0.8% C steel and Invar.

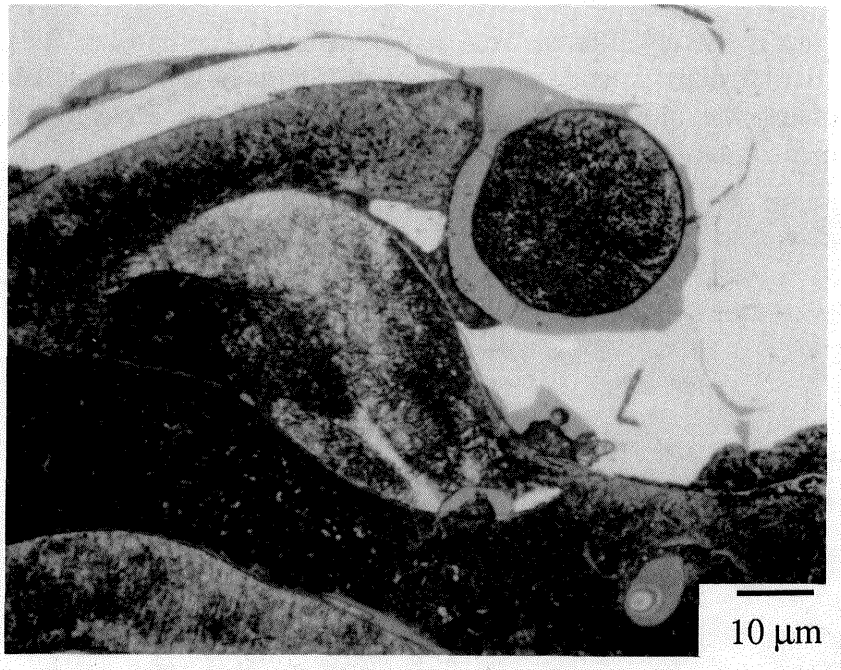

Fig. 13. Detail of interface between 0.8% C steel and Invar in layered composite.

6.2 Pseudo-Alloy In another microstructure experiment we have created a shell of blended materials. The arc–spray process forms an arc between two feed wires to melt them; it is possible for the two wires to be of very different material. Figure 14 shows a shell made from mixing

0.8% C steel and Invar. The sample in Figure 14 was sprayed using argon atomization gas, a shroud, and a backfill shroud gas of argon.

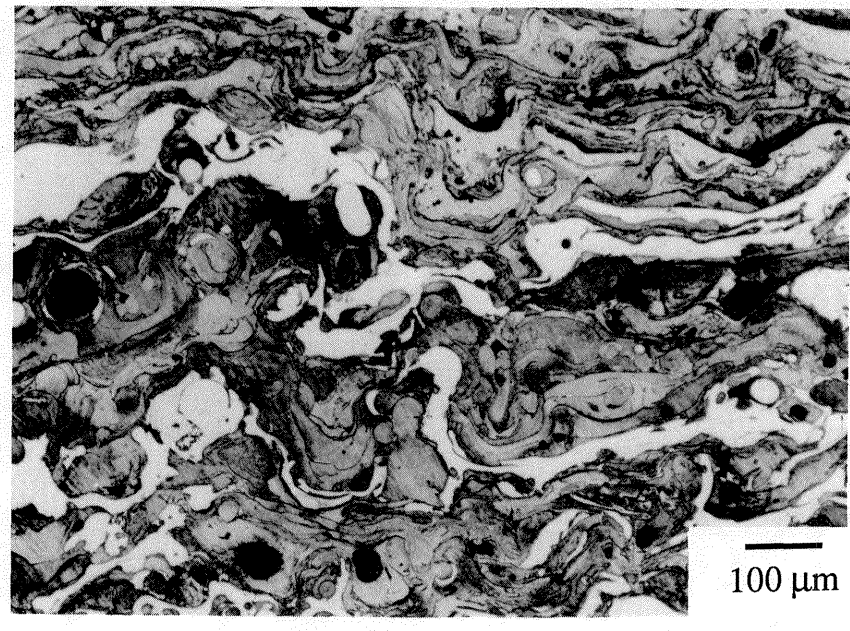

Fig. 14. Mixed pseudo-alloy of 0.8 % C steel and Invar.

The nature of this mix is entirely different from that of the layered composite. The particles arriving molten still form flat lamellæ in the deposit, but the distinct layering of lamellæ is replaced by a random mixture of lamellæ. In Figure 14, the particles are arriving nearly simultaneously, and the bonding of the lamella is similar to that of the layered composite, as seen in Figure 15.

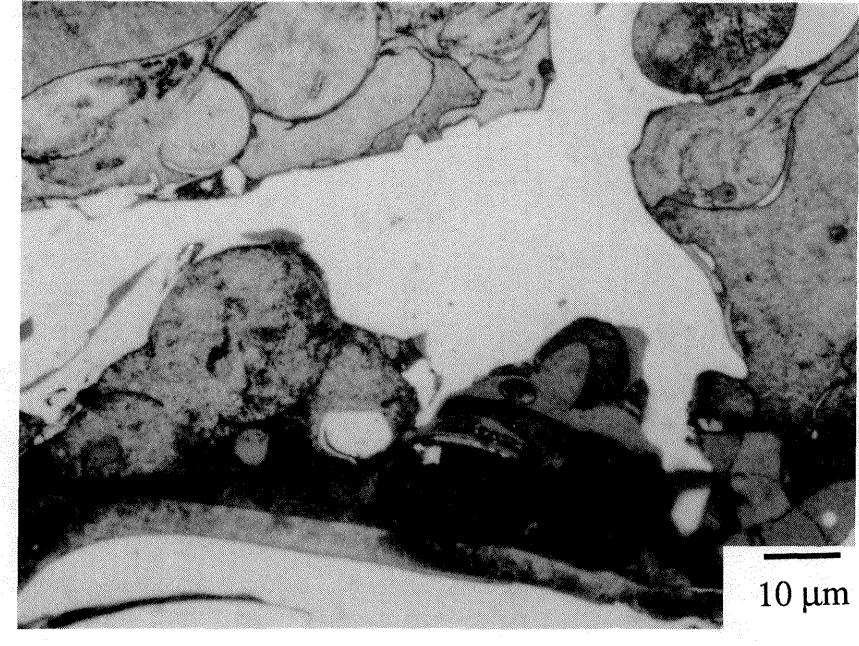

Fig. 15. Detail of inter-lamella region – pseudo-alloy of 0.8 % C steel and Invar.

From the optical micrograph, it is evident that the lamellæ are either Invar or iron. Apparently droplets detach themselves individually either from the steel or the Invar wire feeding the arc, and there is little opportunity for the individual particles to mix either in flight or on the substrate; the solidification rates are sufficient on the substrate to prevent mixing there. X-ray mapping of this deposit has verified that little mixing of the Invar and iron has occurred.

6.3 Oriented Lamellae A shell composed entirely of lamellæ oriented in one direction may show good resistance to stresses in that direction, but will also be weak to stresses applied in other directions. An appropriate control of the orientation of the lamella in a layer will improve the shell's characteristics; this is especially interesting when the orientations and positions of the lamella are designed for specific structural features.

6.3.1 Stratified Orientations The experiment shown in Figure 16 demonstrates a series of stratum, each with a new lamella orientation. The robot was used to systematically apply the material; the lamella are rotated about ±25 degrees from the horizontal. Figure 17 shows a detail of the mixing between the strata. There is mixing of lamella in this region, so there should be good vertical bonding of the strata in the composite structure.

An effort was made in spraying the shell shown in Figure 18 to remove some of the porosity in the shell by mechanically shot peening each layer after it was sprayed. Shot peening also has the effect of changing the state of stress in the shell, but this is not visible in optical metallography. In samples that are made by metal atomized by air, the shot peening also has the effect of removing a measure of the oxide on the surface.

The samples in these figures were sprayed with atmosphere atomization and no shroud. Comparison of Figures 16 and 18 shows that peening the surface between each oriented layer reduces the porosity from 13–15% to 7–9% and reduces the oxide from 34–36% to 30–32%.

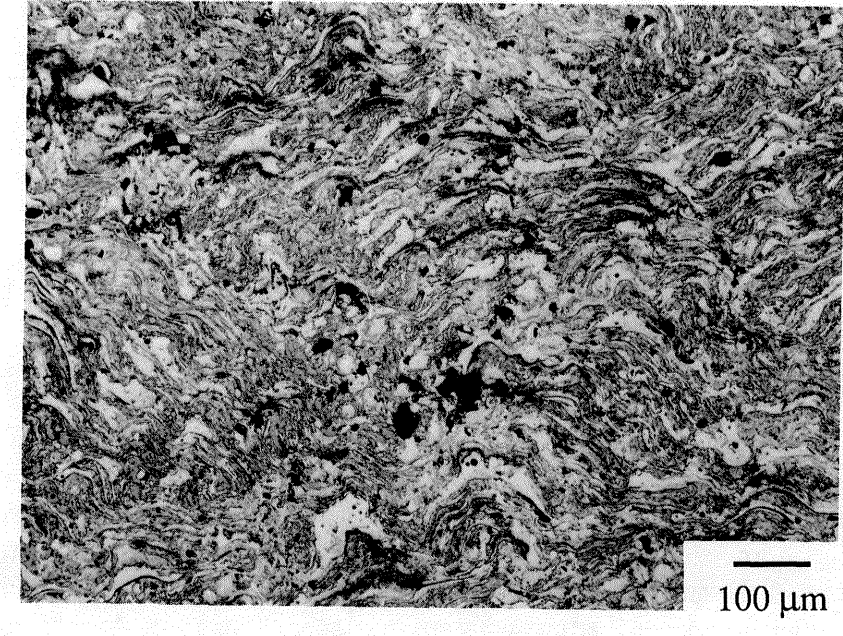

Fig. 16. Oriented lamella of 0.8% C steel.

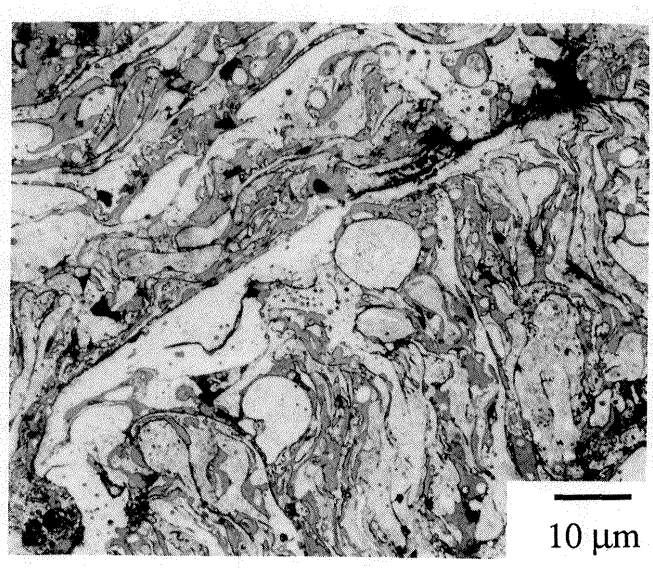

Fig. 17. Detail – oriented lamella of 0.8% C steel.

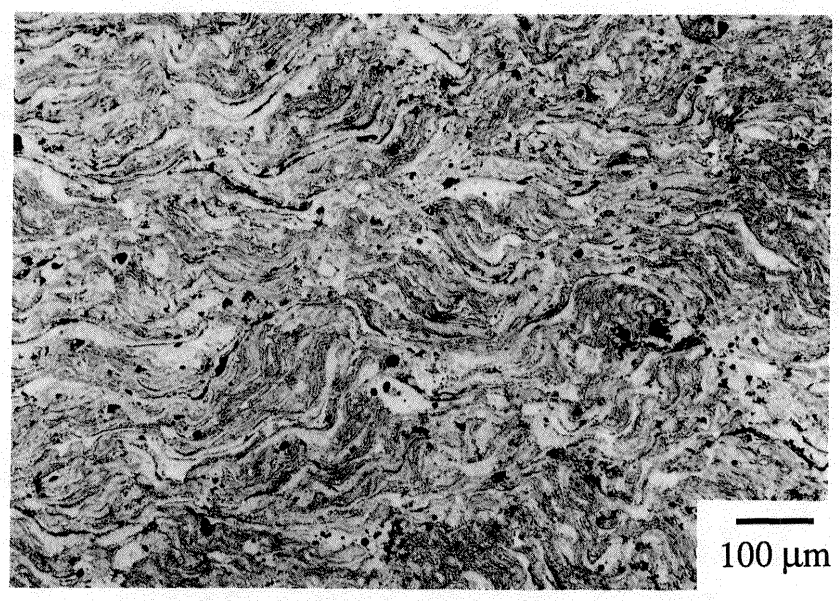

Fig. 18. Oriented lamella of 0.8% C steel with glass peening between each layer.

6.3.2 Flow of Lamella around Features The shells created by metal spraying normally include stress concentrating geometries, particular sharp corners. Arbitrary spraying onto these stress concentrating features of the substrate can create microstructures similar to that in Figure 19. This structure will not withstand corner loading with any measure of success. As a matter of fact, the material in Figure 19 cracked during preparation. Figure 20 shows the same geometry, but a different spray strategy; the lamellæ were oriented to flow over the corner and thus present some

structure to withstand the loading in the corner. Judicious control of the microstructure around asperities, wedges, corners, and similar features is essential for the assuring good mechanical behavior of the shell. The necessary intricate movements of the nozzle over the geometric features of the shell are accomplished most effectively by a robotic manipulator.

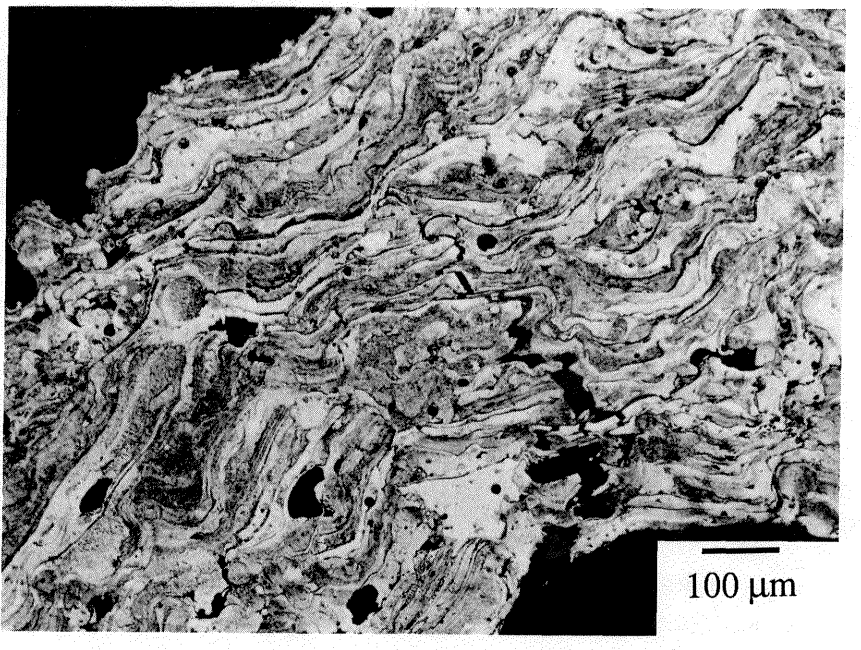

Fig. 19. Lamellæ sprayed around corner.These structures were sprayed using argon atomization without a shroud, in part to highlight the orientation of the lamellæ.

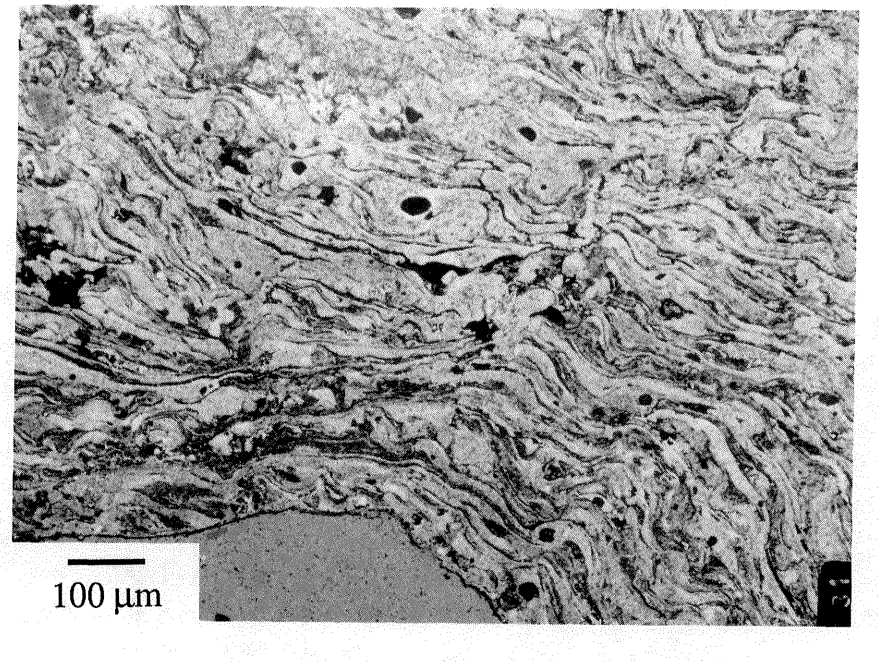

Fig. 20. Flow of oriented lamellæ around corner.

7. CONCLUSIONS

The essence of the result of the arc–spray process is a quilt of quickly solidified lamellæ laced together into a relatively weak structure, a three dimensional jig-saw puzzle. Traditionally, this type of quilt is soaked, and then hot and cold worked to dissolve the impurities; all memory of the porosity and grain boundary imperfections are erased in such processes.

We are applying the arc–spray process to quickly and repeatably create precise shapes — our particular goal is to make tooling shapes for molds. Soaking and working are in conflict with our goals of speed and precision; fortunately the demands of tooling are centered around hoop stresses, compressive loading, and wear. The sprayed metals produce shells that lend themselves to these demands.

To create successful materials in a sprayed shell, we control the levels of oxide. That is, we permit some oxide to remain — these oxides are hard, resist wear well, and are fully supported by the metal matrix surrounding them. We further tailor the microstructure to meet geometry requirements in the shell. Finally, these shells can be composed of composite structures, both in the sense of a variety of materials either mixed together or placed in stratified layers, and in the sense of differing lamella orientations. Consistent creation of this oriented structure is most effectively created by robotically manipulating the spray device.

This work is part of a more comprehensive research effort. The next steps, as guided by this microstructural understanding, must focus on the mechanical behavior of these sprayed materials, paying particular attention to the loading modes and wear conditions that are present in tooling applications. Further work will also concentrate on the failure behavior of these materials in the shells under service conditions; from this information, further design of the material will improve the robustness of the tooling. The result will be insight into the design and fabrication of microstructure and mechanical behavior to give a firm foundation upon which to rapidly build useful sprayed metal shells.

Acknowledgements—This work has been supported by the Alumimum Company of America, by Carnegie Mellon University under a DARPA contract for Shaping by Deposition, and by the Engineering Design Research Center, an NSF Engineering Research Center.

REFERENCES

1. L. E. Weiss, E. L. Gursoz, F. B. Prinz, P. S. Fussell, S. Mahalingam, and E. P. Patrick, *Manufacturing Review* **3**, 40-48 (1990).
2. MOGUL, *Metallizing Manual*, Metallizing Company of America (1963).
3. T. H. Turner and N. F. Budgen, *Metal Spraying*, p. 162, Charles Griffin & Co., London (1926).
4. P. S. Fussell and L. E. Weiss. in *Solid Freeform Fabrication Symposium*, p. 107-113, University of Texas — Austin, Austin, Texas (1990).
5. P. S. Fussell, E. P. Patrick, F. B. Prinz, L. Schultz, D. G. Thuel, L. E. Weiss, K. W. Hartmann, and H. O. K. Kirchner. in *1991 SAE Aerospace Atlantic*, SAE International, Warrendale, PA (1991).
6. E. L. Gursoz, Y. Choi, and F. B. Prinz, in*Geometric Modeling for Product Engineering*, edited by M J Wozny, J U Turner, andK Preiss, Elsevier Science Publishers (1990).
7. S. C. Gill and T. W. Clyne, *Metallurgical Transactions* **21B**, 377-385 (1990).

8. E. J. Lavernia and N. J. Grant, *Materials Science and Engineering* **98**, 381-394 (1988).
9. P. Mathur, D. Apelian, and A. Lawley, *Acta metallurgica* **37**, 429-443 (1989).
10. D. Apelian, M. Paliwal, R. W. Smith, and W. F. Schilling, *International Metals Reviews* **28**, 271-293 (1983).
11. P. Fauchais, A. Grimaud, A. Vardelle, and M. Vardelle, *Annales de Physique* **14**, 261-310 (1989).
12. H. Herman, *Scientific American* , (September) 112-117 (1988).
13. E. Pfender, *Surface Coating Technology* **34**, 1-14 (1988).
14. S. Safai and H. Herman, *Treatise on Materials Science and Technology*, p. 183-214, Academic Press, New York (1981).
15. M. L. Thorpe. in *Thermal Spray Technology: New Ideas and Processes*, ed by D. L. Houck, p. 375-383, ASM International,Metals Park, Ohio (1989).
16. L. Cifuentes and S. Harris, *Thin Solid Films* **118**, 515-526 (1984).
17. S. J. Harris and M. P. Overs, *Thin Solid Films* **118**, 495-505 (1984).
18. S. G. Harris, L. Cifuentes, R. C. Cobb, and D. H. James. in *1st International Conference on Surface Engineering*, p. 79-94, The Welding Institute, Brighton (1985).
19. S. J. Harris, L. Cifuentes, and D. H. James, *Advances in Thermal Spraying*, p. 475-484, Pergamon Press,.New York (1986).
20. J. J. Kaiser and R. A. Miller, *Advanced Materials and Processes* **136**, 37-40 (1989).
21. W. Milewski and M. Sartowski, *Advances in Thermal Spraying*, p. 467-473, Pergamon Press, New York (1986).
22. R. Kawase and K. Maehara, *Journal of High Temperature Society of Japan* **10**, 284-290 (1984).
23. Y. Arata, A. Ohmori, J. Morimoto, A. Yamaguchi, and R. Kawase, *Advances in Thermal Spraying*, p. 485-493, Pergamon Press, New York (1986).
24. C. Moreau, M. Lamoutagne, and P. Cielo. in *National Thermal Spray Conference*, ASM International, Metals Park, Ohio (1991).
25. K. H. Kuo. (editor),*Quasicrystals*, Materials Science Forum, 22–24 (1987).
26. P. J. Steinhardt and S. Ostlund (editors), *The Physics of Quasicrystals*, World Scientific Publishers, Singapore and Teaneck, NJ (1987).
27. D. B. Fowler, W. Riggs, and J. C. Russ, *Advanced Materials and Processes* , November, 41-52 (1990).
28. W. Hume-Rothery, *The Structures of Alloys of Iron*, p. 221, Pergamon Press, New York (1966).
29. M. F. Ashby and D. R. H. Jones, *Engineering Materials 2*, p. 78, Pergamon Press.Oxford (1986).
30. B. Cantor, *Rapidly Solidified Amorphous and Crystalline Alloys*, p. 317-330, B H Kear, B C Giessen, and M Cohen, (editor). Elsevier Science Publishing.Boston (1982).
31. K. Murakami, H. Asako, T. Okamoto, and Y. Miyamoto, *Materials Science and Engineering A* **123**, 261-270 (1990).